

**G. Varughese<sup>1\*</sup>, V. Rini<sup>1</sup>, S.P. Suraj<sup>1</sup> K.T. Usha<sup>2</sup>**

<sup>1</sup>*Department of Physics, Catholicate College, Pathanamthitta, Kerala, India -689645*

<sup>2</sup>*Department of Chemistry, St. Cyril's College, Adoor, Kerala*

\**gvushakoppara@yahoo.co.in*

## **CHARACTERISATION AND OPTICAL STUDIES OF COPPER OXIDE NANOSTRUCTURES DOPED WITH LANTHANUM IONS**

### **ABSTRACT**

Copper Oxide is an extensively studied group II-VI semiconductor with optical properties. It exhibits a wide variety of morphologies in the nano regime that can be grown by tuning the growth habit of the CuO crystal. CuO nano materials with an average particle size of 15-27 nm are synthesized by chemical route. XRD, SEM, FTIR UV-Vis and EDS characterize the samples. The percentage of doping material is confirmed from the EDS spectra. The average crystal size of the prepared CuO: La nanopowder is determined by XRD. The UV absorption spectra revealed the absorption edge at wavelength 389 nm indicating the smaller size of CuO:La nano particle. The optical direct band gap energy of doped CuO nanoparticle is found to be in the range 3.149 eV. The increasing red shift with decreasing particle size suggests that the defects responsible for the intra gap states are primarily surface defect. The La doped CuO is highly effective and can significantly enhance the photo catalytic degradation.

**Key words:** *Nanomaterial, Doping, Optical properties*

### **INTRODUCTION**

Nanomaterials are different from bulk materials and isolated molecules because of their unique optical, electronic and chemical properties [1, 2]. They manifest extremely fascinating and useful properties, which can be exploited for a variety of structural and non-structural applications [3]. Metal oxide nanoparticles belong to a family of nanomaterials that have been manufactured on a large scale for both industrial and household applications, and they hold promise for future applications [4, 5]. Copper Oxide is an extensively studied group II-VI semiconductor with optical properties that permits stable emission at room temperature having immense application in sensors, field emission and photonic devices [6]. Nanoparticles of CuO can be used as gas sensors, optical switch, and magnetic storage media owing to its photoconductive and photochemical properties [7]. Furthermore it is a promising semiconductor for solar cell fabrication due to its suitable optical properties. CuO

nanoparticles have immense medical applications [8, 9, and 10]. It possesses useful photovoltaic and photoconductive properties because CuO crystal structures have a narrow band gap [11, 12]. CuO nanoparticles have been applied in different areas, including sensors catalysis, batteries, high temperature superconductors, solar energy conversion, and field emission emitters [13]. Ohwada K et al. [14] carried out normal coordinate analysis of the optically active vibrations of doped lanthanum copper oxide with the assumption of an infinite  $[(\text{CuO}_2)\text{O}_2]_6$  - layer model. With respect to the results of this analysis, some of the observed bands have been successfully assigned to the Cu-O lattice vibrations. In addition, the force constants concerning Cu-O bonds have also been obtained within the framework of a modified valence force field. It was found that this analysis based on the infinite layer model is useful for assigning the relatively high vibrational frequencies observed at the centre of the first Brillouin zone in doped lanthanum copper oxide. Golosovsky IV et al. [15] demonstrated a noncollinear anti-ferromagnetic structure with the transition temperature of approximately 130 K and propagation vector  $k = [0 \frac{1}{2} 0]$  in the monoclinic compound  $\text{La}_2\text{Cu}_2\text{O}_5$  by using single-crystal neutron diffraction method. They obtained the values and directions of the magnetic moments and crystal structure parameters by least-squares refinement. The results showed that  $\text{La}_2\text{Cu}_2\text{O}_5$  possess low-dimensional magnetic behavior with critical index  $\beta = 0.228(8)$ , like rare-earth cuprates  $\text{R}_2\text{CuO}_4 \cdot \text{La}_2\text{O}_3$  is an ingredient for the manufacture of piezoelectric and thermoelectric material. In is used to increase piezoelectric coefficient and improve product energy conversion efficiency and catalytic applications. Lanthanum is used to improve burning rate of propellant of aircraft. It is a laser material used in X-ray imaging intensifying screens, phosphors as well as in ceramics. Copper oxide nanoparticle has been doped with Lanthanum and studied the effect on energy band gap on doped material [16]. The doping of La ions may enhance optical properties of CuO nano particles. No study on the optical properties of CuO: La was reported so far. Hence the effect of doping La with CuO nanoparticles was studied in this paper.

## EXPERIMENTAL

### Synthesis and characterization

CuO nanoparticles are prepared by Chemical precipitation route. CuO nanoparticles are prepared from copper nitrate solution and ammonia. In this method one molar solution of  $\text{Cu}(\text{NO}_3)_2$  is prepared. For this, 24.16gm of copper nitrate is taken and dissolved in 100ml distilled water. Mix 25ml ammonia solution in 75ml water. These two solutions are kept in two burettes and drop simultaneously into a conical flask containing water and stirred. 0.1M Lanthanum dioxide solutions is dropped along with other two solutions. A precipitate is formed which is washed off using distilled water and acetone. In order to prevent agglomeration 4-5 drops of Tri Ethyl Amine (TEA) was added to solution. After proper centrifugation the residue is dried at  $80^\circ\text{C}$  for one hour in the temperature controlled furnace. Annealing at  $250^\circ\text{C}$  for two hours gives copper oxide. When colour of the sample becomes coffee brown CuO doped with Lanthanum ions is formed.

The orientation and crystallinity of the powder were studied using Rigaku DMAX diffractometer using Cu -K $\alpha$  radiation monochromatised with a graphite crystal and high temperature attachment in  $\theta$ -2 $\theta$  geometry. The surface topography and microstructure were studied using Field Emission Scanning Electron Microscopy (FESEM). Perker Elmer Lamda 25 UV-Vis spectrometer was used to study the optical properties of nanopowder. FTIR spectroscopy uses Michelson interferometer to produce an interferogram. Energy Dispersive X-ray Spectrum Analysis (EDAX) was used to determine percentage composition of La in CuO.

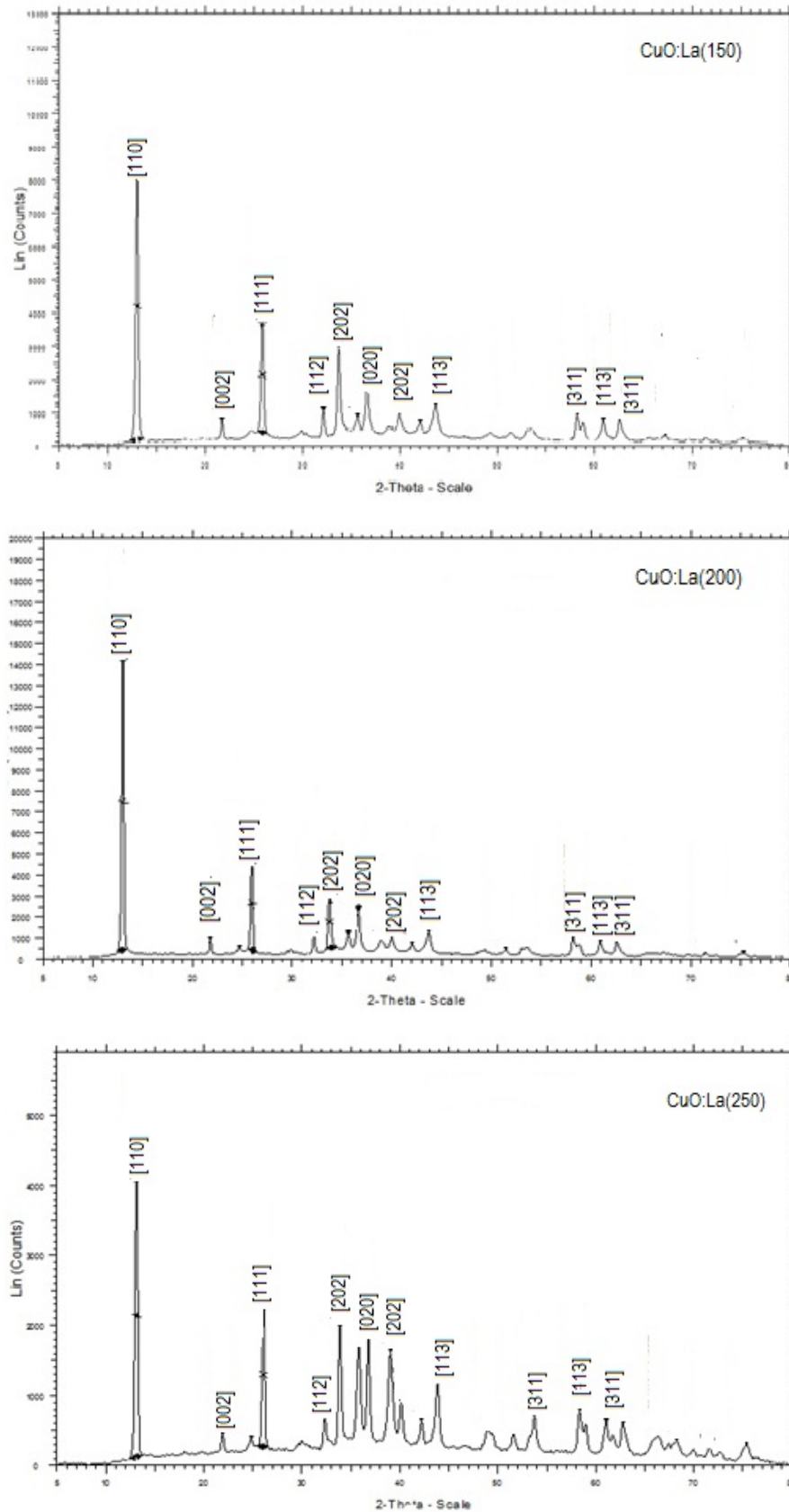
## RESULTS AND DISCUSSIONS

### Characterization using XRD

The XRD pattern, Figure 1(a-c), consists of sharp intense peaks of CuO:La which confirms the good crystalline nature of CuO and peaks originated from (100), (002), (101), (102), (110), (103), (112), (201), (200) and (202) reflections of hexagonal CuO [5]. The XRD techniques are widely used for the particle size and structure determination of nanoparticles. The patterns are compared with JCPDS file No: 80-0075 comparing the observed data with the JCPDS file. The percentage variation of hkl values are shown below in the Table 1. From the table it is noted that percentage variation of hkl values very small, which indicates the change in monoclinic structure of the CuO nanoparticle with doping of La ions is insignificant.

**Table 1.** Comparison of the observed data with the JCPDS file of Copper Oxide. Percentage Variation of d values of nanocrystalline CuO:La annealed at 250°C

Sl No	Observed Value of CuO:La nanoparticle	Standard d-value of CuO nanoparticle	h k l	2 $\theta$	% variation ( $\times 10^{-3}$ )
1	3.44106	3.44400	111	25.871	0.853
2	2.78219	2.72300	400	32.147	0.0217
3	2.68859	2.63500	410	33.685	0.0203
4	2.45244	2.42900	420	36.616	9.567
5	2.14768	2.13300	331	42.037	6.882
6	1.77636	1.7880	610	51.397	6.510
7	1.70950	1.72500	441	56.564	6.682
8	1.5834	1.57300	402	58.22	6.6115

**Determination of particle Size from XRD Pattern of CuO:La****Fig. 1 (a-c).** XRD pattern of CuO:La at 150,200,250°C

The degree of crystallinity of nanoparticles increases with annealing temperature. The percentage of lattice contraction with annealing temperature can also be studied using X-ray diffraction pattern. Particle Size, can be calculated by the formula [9]

$$\text{Debye-Scherrer's formula } D = K\lambda / \beta \cos\theta \quad (1)$$

$K = 0.89$ ,  $\lambda$  the X-ray wavelength = 0.154095 nm,  $\beta$  the full wavelength at half maximum and  $\theta$  the half diffraction angle. The crystal size of CuO: La nano particle at 150,200,250°C was calculated from FWHM and tabulated in Table 2.

**Table: 2.** Particle size measurements of CuO:La from XRD data

Temp (°C)	FWHM	$\beta \times 10^{-3}$	$2\theta$	$\theta$	Particle size (D) Nm
150	0.343	5.98	13.35	6.535	23
200	0.295	5.14	12.892	6.446	27
250	0.24	4.18	12.948	6.474	33

### Variation of Particle size of CuO:La Nanoparticle with temperature

It was found that the crystallite size of CuO: La nanopowder was 23 nm at 150°C which increased to 27 nm at 200°C and 33 nm at 250°C. From the figure it is clear that the intensity of crystalline peaks increases with increase in temperature. Simultaneously the peaks become narrower as the temperature was increased showing the increase in crystallite size. The continuous increase in the particle size with temperature can be attributed to the atomic diffusion. From the atomic perspective, diffusion is a stepwise migration of atom from lattice site to lattice site. In fact, the atoms in solid material are in constant motion, rapidly changing position. For an atom to make such a move the atom must have sufficient energies to break bonds with its neighbor atoms and then cause some lattice distortion during the displacement. As the temperature increases the atom gains sufficient energy for diffusion motion and thereby increasing crystallite size [18]. According to Ostwald ripening phenomena the increase in the particle size is due to the merging of the smaller particles into larger ones as a result of potential energy difference between small and large particles and can occur through solid-state diffusion [17].

### Scanning Electron Microscopy (SEM) of CuO:La

The Scanning Electron Micrographs of CuO: La, Fig.2, nanomaterials synthesized under aqueous medium. The SEM image of CuO: La nanoparticle under high magnification is shown below. Spherical shaped morphology is observed in the micrograph of CuO: La, Fig. 2. The SEM pictures show distinguished spherical morphology with self aligned prismatic nanoparticles. The morphology of CuO nanopowder as revealed by FESEM showed nanoparticle of size 15-100 nm.

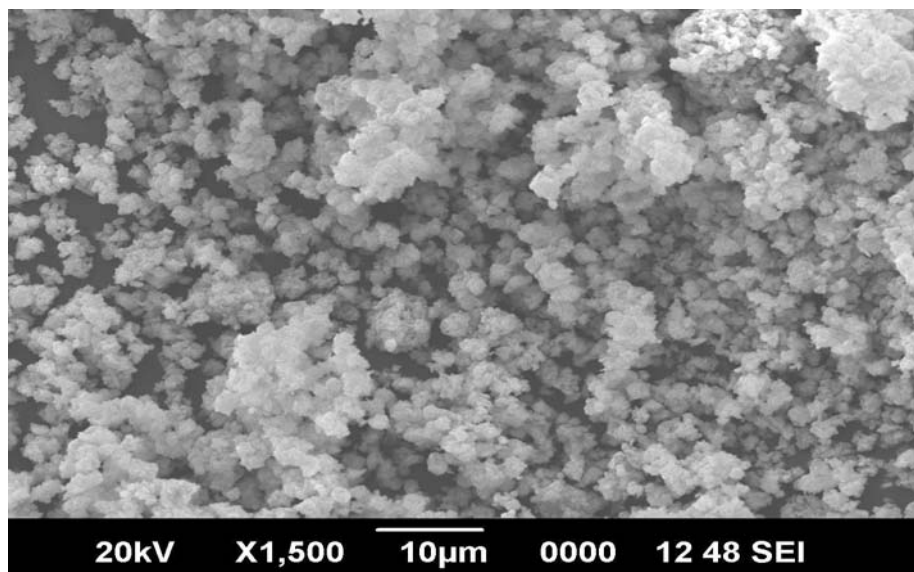


Fig. 2. SEM Image of CuO:La nanoparticle under high magnification

### Energy Dispersive Spectrum Analysis (EDS) of CuO: La nanoparticles

EDAX spectrum, Figure 3, plot not only identifies the elements corresponding to each of its peaks, but the type of X-ray to which it corresponds as well. The higher a peak in a spectrum, the more concentrated the element is in the spectrum. Spherical shaped morphology is observed in the micrograph of CuO:La.

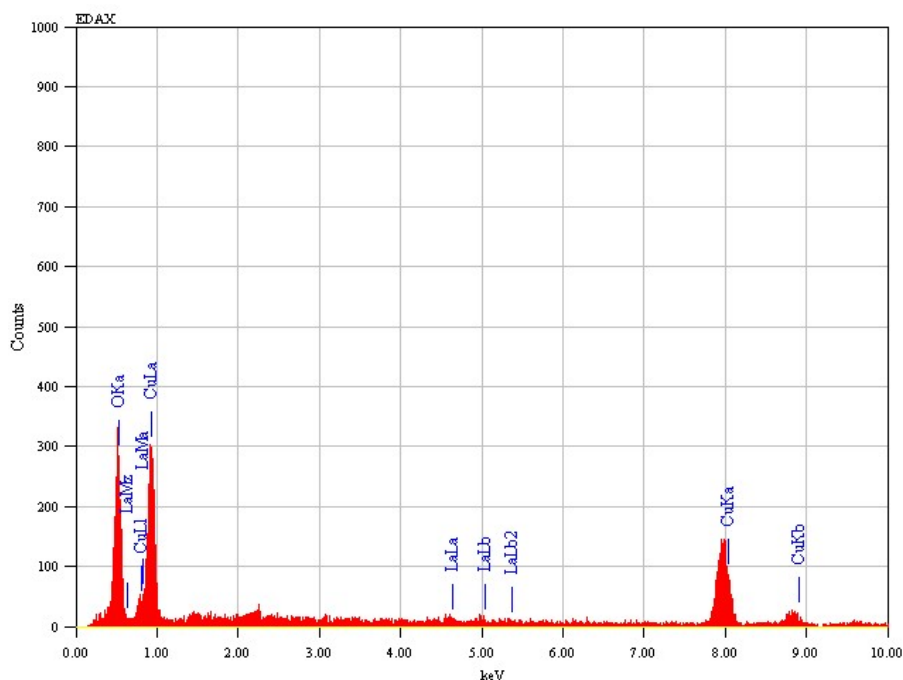


Fig 3. EDAX of CuO: La nanoparticle

The dried powder of the sample was analyzed on Energy Dispersive X-ray Analysis (EDAX or EDS) technique. The peaks have confirmed the presence of Copper, Oxygen and Lanthanum atoms. The average atomic weight percentage ratio of Cu, O, and La in CuO:La

nanoparticle was 31.17: 67.01: 4.648. The energy ratio (in keV) of the elements were 31.37: 0.525: 4.68. The data's are presented in the Table 4. The presence of doped rare earth element Lanthanum ions in CuO nanopowder was confirmed by the analysis.

**Table 4.** Composition of elements in CuO:La sample

Sample	Element	Atomic percentage	Energy (keV)
CuO:La	Cu	31.17	31.37
	O	67.01	0.525
	La	4.68	4.68

### FTIR Spectrum of CuO: La

FTIR spectroscopy uses Michelson interferometer to produce an interferogram and the spectrum of CuO: La is shown in the Fig. 4. It has been shown that as particle size decreases, increase in frequency for the bond (blue shift) is observed in nanoparticles. Bands at  $416.35\text{ cm}^{-1}$  and  $599.23\text{ cm}^{-1}$  are assigned to the stretching vibrations of Cu-O. The stretching frequency of bulk CuO is  $424\text{ cm}^{-1}$ . Here a blue shift is observed in that frequency i.e., that frequency due to quantum confinement. Three intense bands were centered at  $1384.34\text{ cm}^{-1}$ ,  $1041.54\text{ cm}^{-1}$  and  $1556.58\text{ cm}^{-1}$  and are attributed to the stretching vibrations of C = O, C = C and C-H groups in acetate species, which suggests its presents as absorbed species in the surface of nanoparticles. The broad absorption peak centered at  $3423.61\text{ cm}^{-1}$  and  $1626.40\text{ cm}^{-1}$  corresponds to O-H stretching and bending frequencies of  $\text{H}_2\text{O}$ , indicating the existence of water in the surface of nanoparticles [19]. Variations of the peak positions of CuO:La relative to undoped CuO [27,28] are presented in the Table 3. From the data's presented in the table revealed that the doping with lanthanum ions induces a shift in the absorption bands of the undoped CuO.

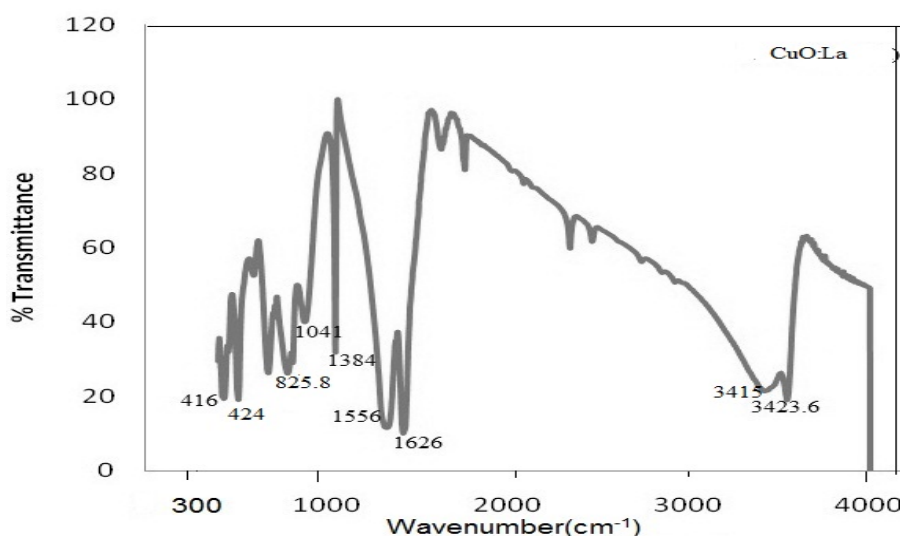


**Fig. 4.** FTIR Spectra of nanocrystalline CuO:La

The peak observed at  $825.80\text{ cm}^{-1}$  may be the presence of some La in the Copper Oxide nanoparticle. The broad absorption peak centered at  $3415.73\text{ cm}^{-1}$  corresponds to O-H stretching of water indicating the existence of water in the surface of nanoparticles [20]

**Table 3.** Comparison of Vibrational modes of undoped and La doped CuO nanoparticle

CuO ( $\text{cm}^{-1}$ )	CuO:La ( $\text{cm}^{-1}$ )	Vibrational modes
3573	3423.61	OH
3486	3415.73	N-H vibration of amine group
2361	2822	O=C=O vibration
1319	1384.34	C=O Stretching
1112	1041.54	C=C stretching
	1626.4	OH deformation
1634	1556.58	C-H
984	825.8	La-O stretching vibrations
606	599.23	Stretching of CuO
432	424	Stretching of CuO
426	416.35	CuO stretching

### UV Absorption and Reflection Spectra

The optical absorption spectrum [21] was used to study the optical properties of the synthesized CuO nanoparticles; from this the band gap and the type of electronic transitions were determined. When a semiconductor absorbs photons of energy larger than the gap of the semiconductor, an electron is transferred from the valence band to the conduction band there occurs an abrupt increase in the absorbency of the material to the wavelength corresponding to the band gap energy. The relation of the absorption coefficient ( $\alpha$ ) to the incidental photon energy depends on the type of electronic transitions. When in this transition, the electron momentum is conserved, the transition is direct, but if the momentum does not conserve this transition it must be attended by a photon this is an indirect electronic transition [21]. Energy band gap studies of these materials have been reported using absorption spectra. The fig.5 depicts the optical absorption spectrum of CuO:La nanopowder prepared under aqueous conditions. The UV visible spectra displayed excitonic absorption peak at 280 nm. It shows that the absorption edge at 389 nm. The material is reported as direct band gap material. For higher values of absorption coefficient, optical absorption shows a power load dependence on photon energy.

### A. Determination of Band gap energy from UV absorption Spectra.

Energy band gap studies of these materials have been reported using absorption spectra, Figure 6. The material is reported as direct band gap material. For higher values of absorption coefficient, optical absorption shows a power load dependence on photon energy [21].

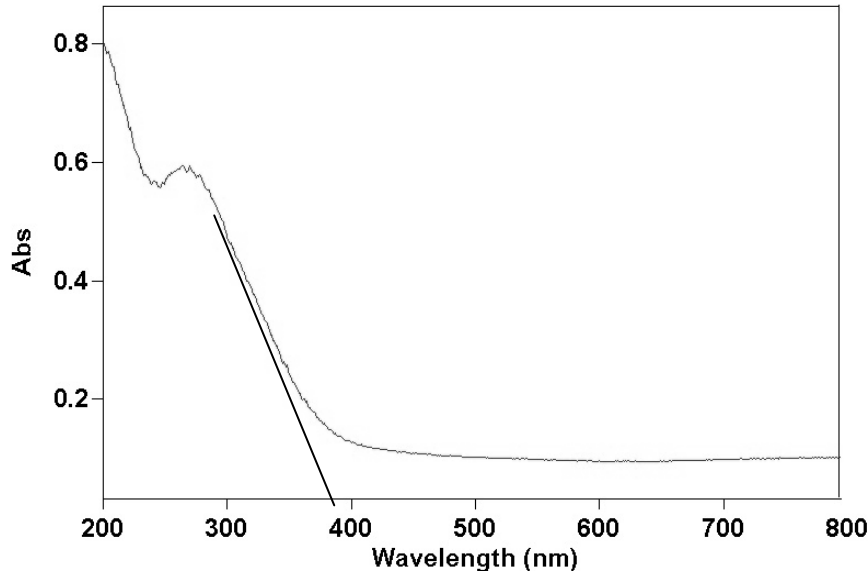
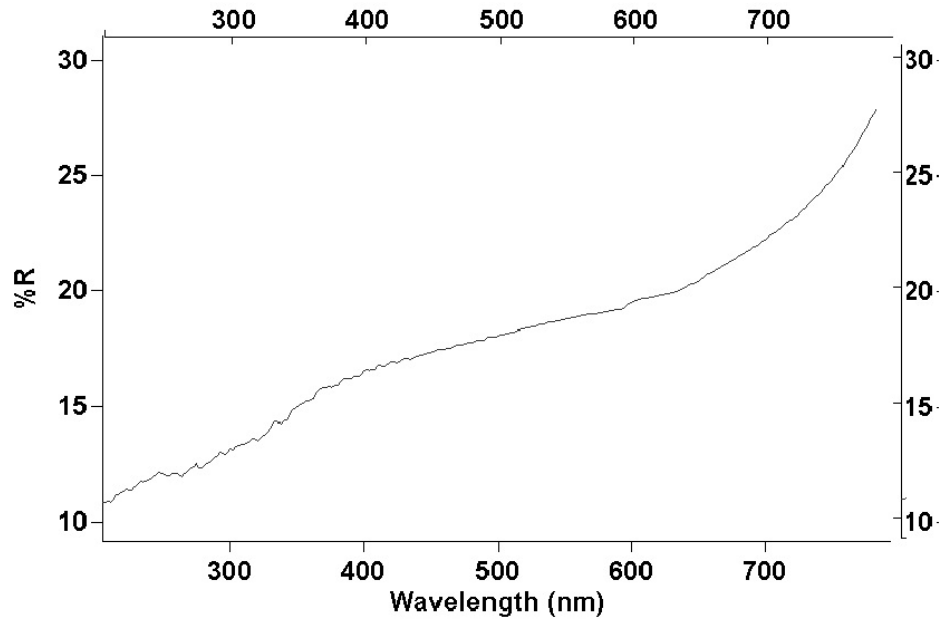


Fig. 5. UV Absorption spectra of CuO: La nanoparticle

$$E_g = h\nu_g = hc / \lambda_g \quad (2)$$

$E_g$  is the optical band gap. Optical energy gap is obtained by extrapolating the linear portion of the absorption spectrum to zero. The energy band gap for La doped CuO is calculated using  $\lambda_g = 389$  nm as 3.149 eV. But the standard band gap energy for CuO nanoparticle is 4.68 eV [23]. On doping band gap energy decreases. Optical absorption shows that the direct band gap versus indirect band gap permits the determination of the crystallinity of a material. Energy band gap studies [22] of these materials have been reported using absorption spectra. The red shift in the band gap energy and reduced electron hole recombination rate make the product material an ideal photo catalyst to harvest solar radiation for various applications. With decreasing particle size, a strong hybridization of the s-p states of the CuO host and the d states of the La impurity is likely to occur [22]. The increasing red shift with decreasing particle size suggests that the defects responsible for the intra gap states are primarily surface defect [25]. The La doped CuO is highly effective and can significantly enhance the photo catalytic degradation. Further these nanoparticles could be used in semiconductor devices such as photo amplifiers, modulators for optical fiber communication system etc. For Copper and oxygen atom paramagnetic and ferromagnetic moments increases with decreasing size. The role of oxygen vacancies is understood to relate to the generation of free carrier mediating ferromagnetism between copper spins [26].

### UV Reflectance spectra of CuO: La



**Fig. 6.** UV Reflection spectra of Cu O: La Nanoparticle

The UV Reflection spectra depicted in Fig. 6 shows a gradual increase in the percentage of reflectance with wavelength.

### CONCLUSION

The size and crystal structure of CuO doped with lanthanum was studied using XRD. The XRD results is indicated that the particle size if nano CuO doped with lanthanum is much small as compared to that of CuO and decreases with lanthanum loading . From XRD results it is clear that as temperature increases, particle size also increases. The change in particle size cause large variation in the physical properties since 1nm size change may introduce a considerable change in the number of surface atoms with lower consideration and broken exchange bonds. The UV absorption spectrum shows a red shift towards 389 nm. The energy band gap for La doped CuO is calculated as 3.149 eV. The increasing red shift with decreasing particle size suggests that the defects responsible for the intra gap states are primarily surface defect. On doping band gap energy decreases. The red shift in the band gap energy and reduced electron hole recombination rate make the product material an ideal photo catalyst to harvest solar radiation for various applications. With decreasing particle size, a strong hybridization of the s-p states of the CuO host and the d states of the La impurity is likely to occur. The La doped CuO is highly effective in enhancing the photo catalytic degradation and could be used as a wide band gap semiconductor.

## REFERENCES

1. Yan L., Zheng Y.B, Zhao F. Li S., Gao X., Xu B. Weiss P.S, Zhao Y, in: Chemistry and Physics of a single atomic layer in Strategies and challenges for functionalization of graphene and graphene-based materials, Chem.Soc.Rev. 41 (2012), 97–114.
2. Amelia, M., Lincheneau C., Silvi S., Credi., in: A. Electrochemical Properties of CdSe and CdTe quantum dots. Chem.Soc. Rev. 41 (2012), 5728-5743.
3. Zheng X.G., Xu C.N., Tomokiyo Y., Tanaka E., Yamada H. and Soejima Y., in: Observation of Charge Stripes in Cupric Oxide, Phys. Rev. Lett. 85 (2000), 5170.
4. Chang M.H., Liu H.-S., Tai C.Y., in: Preparation of Copper Oxide nanoparticles and its application in nanofluid, Powder P.V.D.S. Technol. 207 (2011), 378.
5. Udani P.P.C., Gunawardana Lee H.C., Kim D.H, in: Steam reforming and oxidative steam reforming of methanol over CuO–CeO<sub>2</sub> catalysts, Int. J. Hydrogen Energy 34(2009), 7648.
6. Cao J.L., Shao G.S., Wang Y., Liu Y., Yuan Z.Y., in: CuO catalysts supported on attapulgite clay for low-temperature CO oxidation, Catal. Commun. 9 (2008), 2555.
7. Chiang C.Y., Aroh K., Franson N., Satsangi V.R., Dass S., Ehrman S., in: Copper oxide nanoparticle made by flame spray pyrolysis for photo electrochemical water splitting –Part II. Photo electrochemical study, Int. J. Hydrogen Energy 36 (2011), 15519.
8. [8]Langford J.I. Louer D., High-resolution powder diffraction studies of copper (II) oxide, J. Appl. Crystallogr. 24(1991)149.
9. Abaker M., Umar, A. Baskoutas S., Kim S.H., Hwang S.W., in: Structural and optical properties of CuO layered hexagonal discs synthesized by a low-temperature hydro-thermal process, J. Phys. D: Appl. Phys. 44 (2011), 155
10. Williamson G.K., Hall W.H, in: X-ray line broadening from filed Aluminum and wolfram, Acta Metall. 1 (1953), 22.
11. Moss M.A. Burrell T.S, Ellis G.J., in: Semiconductor Opto-Electronics, Butterworth & Co. Ltd, 1973.
12. Honsi H.M., Fayek S.A., El-Sayed S.M., Roushdy M., in: Optical properties and DC electrical conductivity of Ge<sub>28-x</sub>Se<sub>72</sub>Sb<sub>x</sub> thin films, Vacuum 81 (2006), 54.
13. Sawaby A., Selim M.S., Marzouk S.Y., Mostafa M.A. Hosny A, in: Structure, optical and electrochromic properties of NiO thin films”, Physica B 405 3412 (2010).
14. Ken Ohwade and Ginji Pujiswas in: Optical vibration of doped Lanthanum Copper Oxide compound, Applied Spectroscopy, 47, 3(1993), 296-99.
15. Golosovsky I.V ,Gukasov A.G,Polyakov V.A, in : nonlinear anti-ferromagnetic structure with the propagation vector and the transition temperature of 130K was found in monoclinic compound La<sub>2</sub>Cu<sub>2</sub>O<sub>5</sub> by single crystal neutron diffraction, J Phys-Condensed Matter, 11,36(1999)6959-67
16. Neeleshwar S, Chen C.L, Tsai C.B., Chen Y.Y., Chen C.C., Shyu S.G., Seehra M.S., in: dependent properties of CdSe quantum dots, Phys. Rev. B 71 (2005) 201,307
17. Nanda K K., Kruis F E., Hassan H., Phys.Rev.Lett. 89 (2002) 256103.
18. Gizhevskii B.A., Sukhorukov Y.P., Moskvina A.S., Loshkareva N.N., Mostovshchikova E.V., Ermakov A.E., Kozlov E.A., Uimin M.A., Gaviko V.S in : Anomalies in the Optical properties of Nanocrystalline Copper Oxides CuO and Cu<sub>2</sub>O near the fundamental absorption edge, JETP 102 (2006) 297.

19. Sukhorukov Y.P., Gizhevskii B.A., Mostovshchikova E.V., Yermakov A.Y., Tugushev S.N., Kozlov E.A., in: Nano-crystalline Copper Oxide for selective solar energy absorbers, *Tech. Phys.Lett.* 32 (2006) 132.
20. Ovchinnikov S.G., Gizhevskii B.A., Sukhorukov Y.P., Ermakov A.E., Uimin M.A., Kozlov E.A., Kotov Y., Bagazeev A.A.V, in: Specific features of the electronic structure and optical spectra of nanoparticles with strong electron correlations, *Phys. Solid State* 49 (2007), 1116
21. Rehman S., Mumtaz A Hasanain S.K., in: Size effects on the Magnetic and Optical properties of CuO nanoparticles”, *J. Nanopart. Res.* 13 (2011), 2497.
22. Koffyberg F.P., Benko F.A., in: A Photoelectrochemical determination of the position of the conduction and valence band edges of p-type CuO , *J. Appl. Phys.* 53 (1982), 1173.
23. Neeleshwar S., C. Chen., Tsai L. C.B., Y. Chen., C.Y. Chen., C. Shyu S.G., Seehra M.S., in: Size-dependent properties of CdSe quantum dots, *Phys. Rev. B* 71 (2005), 201307.
24. Sukhorukov Y.P., Gizhevskii B.A., Mostovshchikova E.V., Yermakov A.Y., Tugushev S.N., Kozlov E.A.,in: Nano-crystalline Copper Oxide for selective solar energy absorbers, *Tech. Phys.Lett.* 32 (2006), 132.
25. Ovchinnikov S.G., Gizhevskii B.A., Sukhorukov Y.P., Ermakov A.E., Uimin A., Kozlov E.A., Kotov Y.,Bagazeev A.A.V.,in: Specific features of the Electronic structure and Optical spectra of nanoparticles with strong electron correlations, *Phys. Solid State* 49 (2007) 1116.
26. Koffyberg F.P., Benko F.A.,in: A photoelectrochemical determination of the position of the conduction and valence band edges of p-type CuO , *J. Appl. Phys.* 53 (1982), 1173.
27. Mushtaq A.D,Sang H, in: Synthesis character and Electrochemical properties of CuO nanostructure,*J.Solid state Electrochemical* 14(2010), 1719-26.
28. Kannaki k,Remesh PS, Hydrothermal synthesisi of CuO Nanostructure and their charactgerisation, *In.J. of Scientific & Engg.Res.* 3,9 (2012), 1-4